Carbon Capture from Natural Gas Combined Cycle Power Plants: Solvent Performance Comparison at an Industrial Scale

Mahdi Sharifzadeh and Nilay Shah
Dept. of Chemical Engineering, Centre for Process Systems Engineering (CPSE), Imperial College London, London SW7 2AZ, U.K.

DOI 10.1002/aic.15072
Published online October 26, 2015 in Wiley Online Library (wileyonlinelibrary.com)

Natural gas is an important source of energy. This article addresses the problem of integrating an existing natural gas combined cycle (NGCC) power plant with a carbon capture process using various solvents. The power plant and capture process have mutual interactions in terms of the flue gas flow rate and composition vs. the extracted steam required for solvent regeneration. Therefore, evaluating solvent performance at a single (nominal) operating point is not indicative and solvent performance should be considered subject to the overall process operability and over a wide range of operating conditions. In the present research, a novel optimization framework was developed in which design and operation of the capture process are optimized simultaneously and their interactions with the upstream power plant are fully captured. The developed framework was applied for solvent comparison which demonstrated that GCCmax, a newly developed solvent, features superior performances compared to the monoethanolamine baseline solvent. © 2015 American Institute of Chemical Engineers *AIChE J*, 62: 166–179, 2016
Keywords: CO2, carbon capture, natural gas combined cycle (NGCC) power plant, energy efficiency, integrated process design and control, GCCmax

Introduction

Increasing energy demand and associated pollution have posed an important challenge around the security of energy supply and environmental protection. Among various prospective scenarios, the International Energy Agency (IEA) asserts that fossil fuels are most likely to remain the dominant sources of energy for a foreseeable future.[1] Therefore, carbon capture from existing fossil-fuel-driven energy infrastructure will be a major pathway for sustainability and environmental protection. Despite such clarity, there are various barriers against commercialization of carbon capture technologies. First, the current energy infrastructure is relatively mature and the number of existing processes is significantly larger than the number of processes under construction. Therefore, enhancing energy efficiency and mitigating the emissions should require minimal process retrofit. Second, seamless integration of energy conversion processes with carbon capture technology requires the latter process to be at least as flexible as the former (standalone) process. Finally, to justify the process retrofit and overcome financial barriers, the energetic implications of the carbon capture process should be minimal.

Solvent-based CO_2 removal using aqueous amines is the most promising technology for carbon capture, as this technology is an end-of-pipe treatment and has been in use since the 1930s for natural gas sweetening.[2] However, adaptation of this technology for postcombustion carbon capture is nontrivial as gas processing is significantly different from power generation in several aspects. Natural gas is often produced at an elevated pressure and does not contain any oxygen. Furthermore, in natural gas sweetening, a higher degree of CO_2 removal is required and the separated CO_2 is emitted to the atmosphere. Finally, gas processing is a relatively steady-state process. By comparison, postcombustion carbon removal is conducted at near atmosphere pressure and deep CO_2 separation is often uneconomic. In addition, power plants are subject to drastic variations in electricity demand and for the capture plant to remain integrated with the power plant, it should feature a high degree of flexibility.

Retrofitting the existing power generation processes with carbon capture technologies has been the focus of academic and industrial researchers. The IEA conducted a comparative study[3] on precombustion and postcombustion CO_2 capture in natural gas combined cycle (NGCC) power plants, as well as precombustion carbon capture from coal gasification plants. Postcombustion carbon capture from natural gas was identified as the lowest cost retrofit. Later, the National Energy Technology Laboratory, in a comprehensive study,[4] evaluated the implications of carbon capture from NGCC, integrated gasification combined cycle (IGCC), and pulverized coal (PC) power plants. The observation was that the energetic penalties associated with carbon capture from NGCC power plants are less than PC and IGCC power plants, mainly due to the lower

This contribution was identified by the AIChE Session Chair, Dr Athanasios Papadopoulos (Centre for Research and Technology Hellas), as the **Best Presentation** in the session of **Design of CO_2 Capture Systems** during the 2014 AIChE Annual Meeting in Atlanta, GA, November 16–21, 2014.

Correspondence concerning this article should be addressed to M. Sharifzadeh at mahdi@imperial.ac.uk

carbon intensity of the natural gas and the higher conversion efficiency of NGCC plants. Large increases in the boiler water withdrawal and cooling water were observed for the scenario of NGCC power plant, integrated with carbon capture process. Recently, a group of European researchers[5] conducted a comprehensive study on the carbon capture from a supercritical pulverised coal power plant and a NGCC power plant. They employed two economic analysis methods; a top-down method in which the historical data from previous projects and similar studies were used, and a bottom-up method that was based on mass and energy analysis and detailed equipment costing. Significant difference between the results of two studies was reported (table 7 of Ref. 5), illustrating the difficulties associated with reproducible and comparative economic analysis.

Furthermore, researchers have focused on the method of process integration from a thermodynamic point of view. The heat integration schemes investigated include steam extraction and condensate recycling,[6] integrating compressor intercoolers to the low pressure (LP) section of the steam cycle[7] or stripper reboiler,[8] preheating combustion air using waste heat from the capture plant,[9] and application of pressurized hot water instead of steam for solvent regeneration.[10,11] Furthermore, the CO_2 concentration of the flue gas can be increased by recirculation of exhaust gases[10,12,13] or using a supplementary burner placed in the duct connecting the turbine exhaust and heat recovery steam generation (HRSG) system.[12–14] Other researchers have explored the implications of the process configuration on the capital investment and energy costs.

It was shown that depending on the solvent heat of desorption, either a multipressure or vacuum desorber could be the optimal configuration.[15] Other configurations include the absorber with intercooling, condensate heating, evacuation using water ejector, stripper overhead compression, lean amine flash, split-amine flow to absorber and desorber, and their combinations. Le Moullec et al.[16] classified these configurations into three categories: (1) absorption enhancement, (2) heat integration, and (3) heat pump applications. They enumerated 20 process configurations from the open literature and patents. In general, up to 37% energy saving in terms of the required reboiler steam was reported.[17] Damartzis et al.[18] applied a module-based generalized design framework to optimize process flow diagram including the stream topologies, the heat redistribution and the cascades of desorption columns. They reported significant economic improvement (15–35%) and reductions in the reboiler duty (up to 55%). However, as discussed by Karimi,[19] a high degree of energy integration may result in poor dynamic behavior, because in energy-integrated processes, disturbances propagate in several paths. Therefore, a trade-off between energy saving and process controllability should be established.[20]

Nevertheless, integrated operation of carbon capture processes may not be realizable without considering the main operational characteristics of the upstream power plant. Power plants are subjects to drastic variations in the electricity demand. Examples of such variations include regular daily and hourly variations in the consumer demand or stochastic variations such as extreme weather conditions or local events. It is expected that by the introduction of renewable energy resources, the fluctuations in the electricity grid will also increase on the supply side, as some of these new resources such as solar or wind have intermittent generation characteristics. Thus, it is for the fossil-based power plants to operate flexibly and balance the supply deficit to meet the demand. Therefore, commercialization of new CO_2 capture technologies strongly depends on their adaptability to remain integrated as the upstream power plant experiences variations in the electricity demand. Recently, the flexibility of solvent-based carbon capture processes has been the focus of various research groups. Shah and Mac Dowell[21] studied the multiperiod operation of a coal-fired power plant. They adapted a time-varying solvent regeneration strategy to minimize the costs of CO_2 capture. Delarue et al.[22] had a similar observation that flexible operation of capture plant would offer a better economy. Lawal et al.[23] studied the dynamic performance of carbon capture from a coal-fired subcritical power plant. They concluded that the capture plant has a slower dynamic response than the power plant, which can prolong the power plant start-up or load-change due to steam extraction. In addition, it was observed that the interactions between the control loops in the power plant and capture plant limit the overall process controllability. Bypassing the flue gas, solvent storage and stripper-bypass can potentially offer flexibility and economic savings.[24,25]

In the present article, we explore model development and validation, scale up, NGCC power plant integration and flexible operation of the capture processes. The research questions also include the interactions between the power plant and carbon capture plant in terms of the flow and composition of the flue gas and the required steam for solvent regeneration, which have implications for the overall energy efficiency and operational flexibility. The performances of GCCmax and the monoethanolamine (MEA) solvents for carbon capture from an NGCC power plant are studied. GCCmax is recently developed by Carbon Clean Solutions Limited (CCSL) and belongs to the class of amine-promoted buffer salt (APBS) solvents. MEA is chosen as the reference solvent for comparison. Nevertheless, the research methodology is general in nature and can offer effective standards for carbon capture solvent development and comparison.

In the following sections, first, the overall process block diagram and the process flow diagram of the subprocesses are presented and discussed. Then, the capture process model is briefly discussed and justified. The discussions continue with the implications of various operating modes of the combined cycle gas turbine (CCGT) for the flue gas flow rate and composition. These enable the application of an optimization framework for the problem of retrofitting an existing NGCC power plant using solvent-based capture process. Finally, conclusions are made with respect to the implications GCCmax and MEA reference solvent in terms of technical and energetic performance measures.

Overall Process Block Diagram

The overall process block diagram is shown in Figure 1. As shown in this figure, the NGCC power plant comprises two trains of CCGT, HRSG systems that are integrated to the steam turbines at three high pressure (HP), medium pressure (MP), and LP levels. The advantages of parallel trains are due to the fact that in the presence of large variations in the electricity demand, it is possible to shut down a gas turbine and operate the other train close to its nominal operating conditions, that is, at a high conversion efficiency. Based on a similar justification, in the present research, separate carbon capture and compression trains are considered in the downstream process, to enable flexible operation of the overall integrated process. Figure 1 shows that the NGCC power plant integrates with the carbon capture plant at three points. The

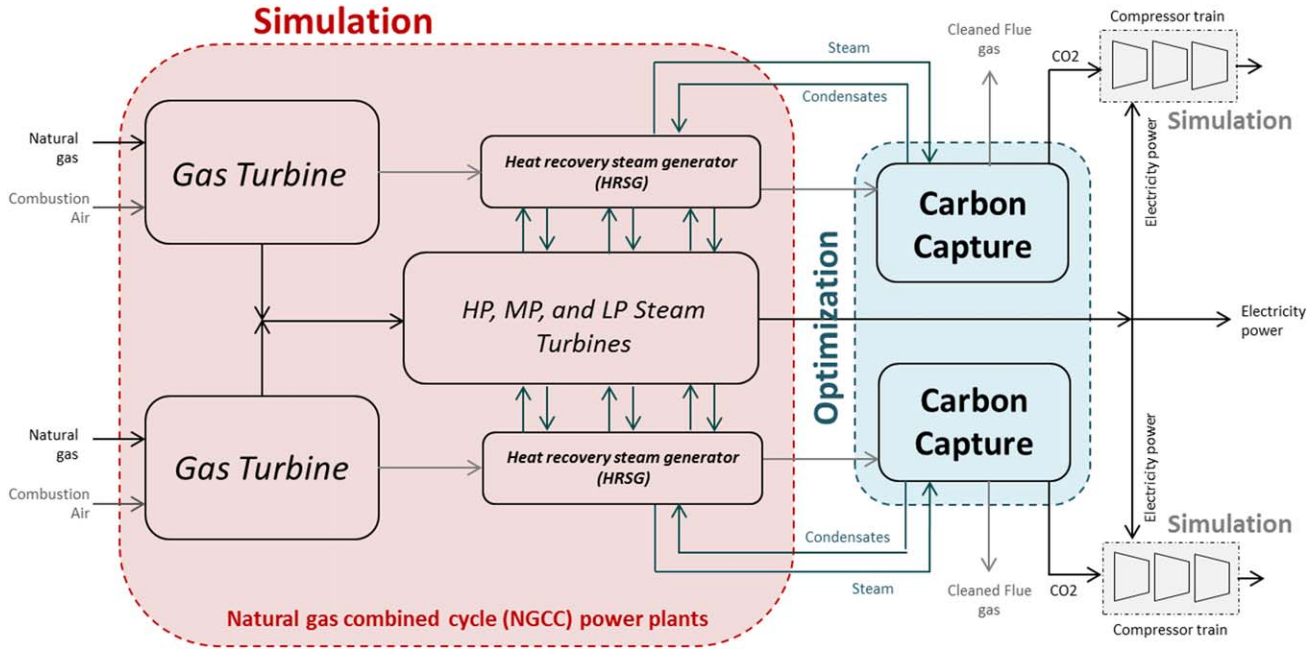

Figure 1. The block diagram for a NGCC power plant integrated with CO_2 capture and CO_2 compression processes.

[Color figure can be viewed in the online issue, which is available at wileyonlinelibrary.com.]

flue gas is sent from the power plant to the capture plant for CO_2 separation. In addition, the capture plant relies on the steam from the power plant for regeneration of the solvent and it returns the condensates to the power plant for reuse and further steam generation.

Process flow diagram of NGCC power plant

Figure 2 shows the process flow diagram of the NGCC power plant, in more detail. This process consists of three subprocesses, CCGT, HRSG system, and stream turbines at HP, MP, and LP levels. First, air is compressed and fed to the combustor where natural gas feed is burned to release heat. Hot exhaust gases are expanded in the gas turbine to produce electricity. Then, the hot gases are exploited in the HRSG for generating steam at the three pressure levels. The steam from the HP steam drum is sent to the HP steam turbine. The discharge of HP turbine is mixed with the steam from the MP steam drum and is superheated in the economisers before entering the MP steam turbine. The discharge of the MP steam turbine is mixed with the steam generated at the LP steam drum. A fraction of this steam stream is extracted and sent to the reboiler of the CO_2 capture plant for solvent regeneration. The pressure and temperature of the extracted steam is adjusted in the desuperheater using the condensates returning from the capture plant. In addition, a valve before the LP steam turbine ensures that the extracted steam is at the desired pressure. Both HP and MP turbines are of the back-pressure type. However, the LP turbine is a condensing turbine. The justification of using a condensing turbine is that the produced power is proportional to the pressure ratio between suction and discharge. Therefore, it is possible to enhance the produced work by creating vacuum conditions at the turbine discharge using a surface condenser. The condensates from the surface condenser and the condensates returning from the carbon capture plant are mixed, deaerated, pressurized, and recycled to the steam drums for further steam generation.

Process flow diagram of CO_2 capture and compression sections

Figure 3 shows the process flow diagram of the CO_2 capture and compression sections. In the first column, the flue gas from the power plant comes into direct contact with cooling water to reduce its temperature and remove any entrained particles. In the next column, absorber, the CO_2 is chemisorbed and removed by the solvent. The CO_2-rich solvent leaves from the absorber bottom, and the cleaned flue gas exits from the absorber top and is sent to the water wash column. The aim of the water wash column is minimizing the solvent loss by absorbing the solvent spilled from the top of the absorber. The CO_2-rich solvent from the bottom of the absorber is sent to the top of the desorber for CO_2 stripping and solvent regeneration. The CO_2-lean solvent from the desorber reboiler is recycled to the absorber for reuse and CO_2 separation. The absorption reactions are exothermic and favor low temperatures. By comparison, the desorption reactions are endothermic and favor high temperatures. Therefore, there is an opportunity for heat integration between hot CO_2-lean and cold CO_2-rich streams. The separated CO_2 from the desorber condenser is sent to the compression section. The compression section consists of seven compression stages. In each compression stage, due to pressure enhancement, the temperature of the CO_2 gas is increased, and needs to be cooled in the subsequent interstage cooler. As a result of sequential compression and cooling, most of the water content is condensed in the early stages. The remaining water is removed using an adsorption process in the dehydrators. The compressed CO_2 is sent from the last stage for storage and sequestration.

Research Methodology

For the capture plant, the details of model development, pilot plant trials, and model validation were reported in a

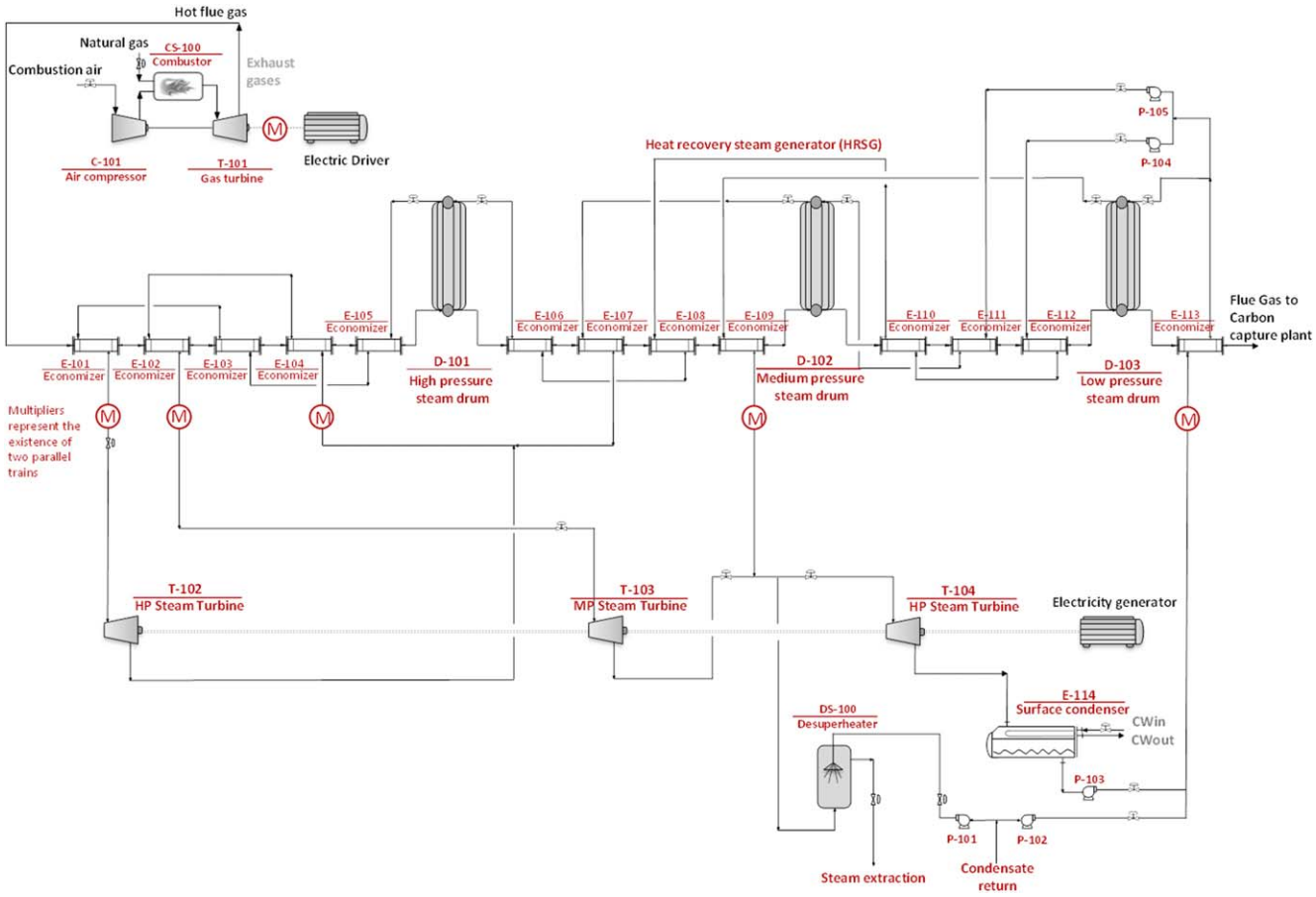

Figure 2. The process flow diagram of the NGCC power plant.

[Color figure can be viewed in the online issue, which is available at wileyonlinelibrary.com.]

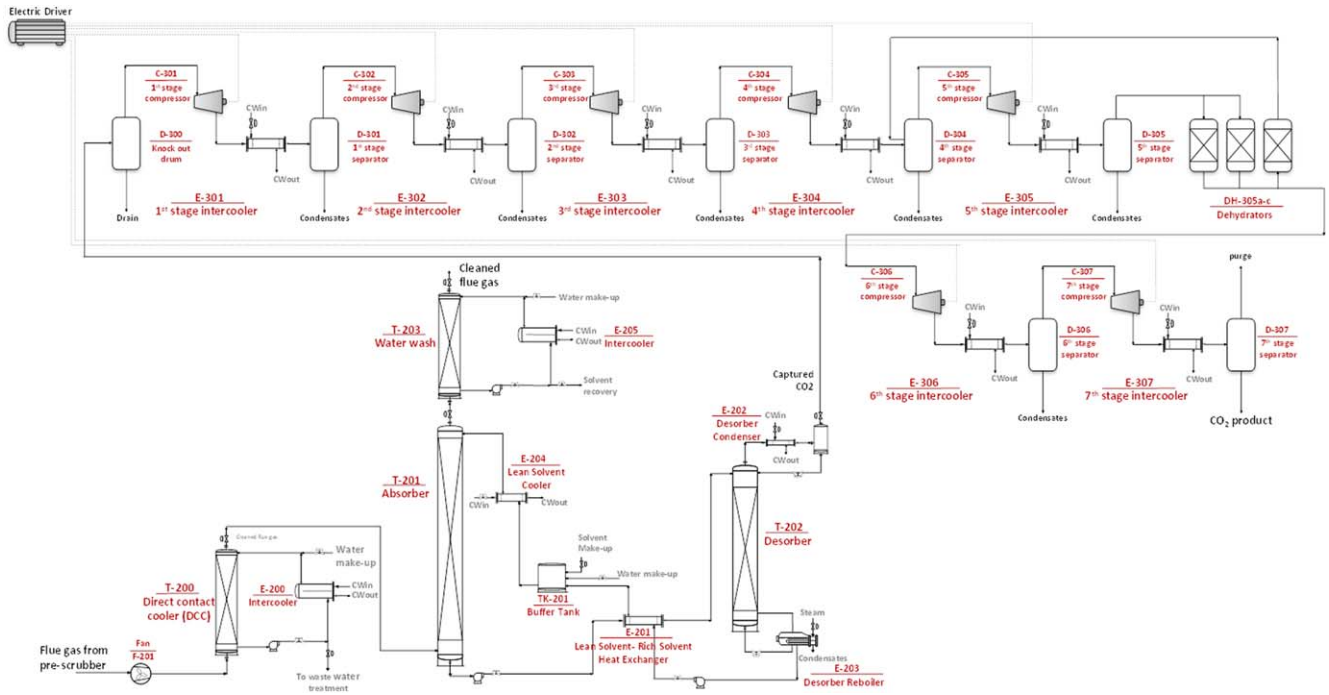

Figure 3. The process flow diagram of the CO_2 capture and CO_2 compression processes.

[Color figure can be viewed in the online issue, which is available at wileyonlinelibrary.com.]

previous contribution.[26] The present research builds upon this initial results and aims at evaluating the performance of the GCCmax solvent in comparison with the MEA benchmark solvent, at an industrial scale and when integrated to an NGCC power plant. In the following, first, the problem statement for retrofitting an NGCC power plant with carbon capture and compression processes is presented. Then, model development and validation are briefly discussed. Then, the capture process model is scaled up and integrated to the power plant model. The main feature of interest is uncertainties in the power plant electricity demand that require flexible operation of the capture process to realize seamless process integration and retrofit. A novel optimization framework is proposed to address the posed retrofit problem. In the proposed optimization framework, the design and operation of the capture process are optimized simultaneously, and the interactions of the down steam capture process with the upstream in terms of the flue gas flow rate and composition and the required steam for solvent regeneration, as various electricity load scenarios are fully considered. Then, the implementation software tools are elaborated upon. Finally, the results are reported and discussed.

Problem statement

The present research addresses the problem of retrofitting an existing NGCC power plant using solvent-based carbon capture and compression processes. The specifications of an existing NGCC power plant including the nominal operating conditions and the performance curves of process equipment under various partial load scenarios are given. It is intended to retrofit the power plant with CO_2 capture and compression plants, so that 90% of the CO_2 from natural gas combustion is captured and compressed to 111 bar for subsequent storage and sequestration. In addition, it is desired to ensure that the capture plant and its compression network remain operable at a wide range (i.e., 25–100%) of electricity power demands.

Capture plant model development and validation

The accurate modeling of the solvent-based CO_2 capture processes for the purpose of solvent benchmarking and comparison requires a thorough understanding of the underlying physical and chemical phenomena involved, as discussed in the following.

Rate-based modeling of gas–liquid contactors (GLC)

The rate-based model of the GLC is founded on the two-film theory. In this method, thermodynamic equilibrium is assumed only at the interface of vapor and liquid phases. Unlike equilibrium-based models, the exiting vapor phase is superheated and the exiting liquid phase is subcooled and they have different temperatures. The exchanged mass and energy between phases depend on the driving forces, transport coefficients, and the interfacial area. Often, both convective and diffusive transport phenomena are involved and component-coupling effects need to be considered.[27] Various empirical correlations for calculating the mass transfer coefficient are proposed by researchers for random[28–30] and structured packing.[30–32] Finally, the bulk liquid and gas phases may have different flow configurations such as plug or mixed flows.

Reaction kinetics and thermodynamics

In the present research, the statistical associating fluid theory (SAFT) was adopted for modeling the chemical and phase equilibria. In this approach, the rate of reactions, the concentration of intermediate ionization species, and their thermophysical properties are not formulated directly. Instead, CO_2 and solvent are represented as molecule chains with associating sites. The concentration of CO_2 in association with the solvent molecules represents the actual CO_2 loading at different temperatures and pressures.

Justification of the modeling strategy

The combination of rate-based modeling and representation of chemical reactions using SAFT provides a consistent modeling approach. The justification is that for solvents such as MEA and GCCmax, the rate of reaction is significantly faster than the heat and mass transfer rates. Therefore, the knowledge of the reaction kinetics is unnecessary and chemical equilibrium sufficiently describes the actual system behavior at the gas-liquid interface. This modeling approach offers several advantages; first, unlike activity-based models, the same equation of state is used to describe both liquid and vapor phases. Second, the chemical equilibria are treated at the same level as phase equilibria. Furthermore, this approach results in significant model reduction because the speciation of intermediate ions is not included in the mathematical formulation and the uncertainties associated with their thermophysical parameters are disentangled from problem formulation. Most of all, the aforementioned approach establishes a connection between the chemical and physical behavior of the mixture and the molecular structure of the involved materials. This is of particular importance to modeling new solvents as the required information can be acquired from the available data for the molecular segments of associating sites.

In the present research, the applied software tools were advanced modeling library gas-liquid contactors (AML-GLC) and gSAFT toolboxes developed by Process System Enterprise (PSE). The parametric values of thermodynamic models for the GCCmax solvent are obscured to respect the confidentiality agreements with CCSL and PSE. The modeling equations of the GLC and the underlying assumptions are described in.[33] More details on the thermodynamic model are given in Ref. 34.

Pilot plant studies and model validation

As discussed in a previous contribution,[26] to ensure effective benchmarking and model validation, two sets of pilot plant runs were conducted using the MEA and GCCmax solvents. MEA served as the baseline reference solvent. The pilot plant studies were conducted in the US National Carbon Capture Center (NCCC) located in Alabama. Table 1 shows the results of model validation for MEA reference solvent.[26] As the US NCCC pilot plant was not previously operated under natural gas exhaust conditions, the model validation was conducted based on historical data for a scenario of coal-fired exhausts. The last column in Table 1 reports the prediction of the model, when the system is operated for natural gas exhaust conditions. Table 1 shows a very good agreement between pilot plant data and simulation results, in terms of the captured CO_2 and the solvent composition. Minor discrepancies in the consumed steam are deemed to be associated with heat losses and temperature indicator errors. Table 2 reports the results of the GCCmax solvent model validation under natural-gas-fired conditions.[26] Two sets of pilot plant data were used, which are different with respect to the lean solvent temperature entering the absorber top. The justification was due to the fact that in

Table 1. Model Validation for MEA Baseline Solvent[26]

		Alabama Coal	Alabama Coal	Alabama NG
		Pilot Plant	Simulation	Simulation
Flue gas to the absorber				
Nitrogen + Oxygen	Mass fraction	0.786	0.786	0.909
Carbon dioxide	Mass fraction	0.165	0.165	0.067
Water	Mass fraction	0.049	0.049	0.024
Total flow rate	kg/s	0.6279	0.6280	0.6279
Flue gas temperature–Absorber inlet	K	316.56	316.56	316.56
Lean solvent–absorber inlet				
Amine	Mass fraction	0.297	0.298	0.296
CO_2	Mass fraction	0.063	0.059	0.059
Water	Mass fraction	0.640	0.643	0.645
Total	kg/s	2.5200	2.5100	1.3000
Lean solvent temperature	K	316.15	316.15	316.15
Intercoolers outlet temperature	K	316.15	316.15	–
Reboiler steam				
Steam pressure	bar	2.92	2.92	2.92
Steam temperature	K	405.60	405.60	405.60
Steam flow rate	kg/s	0.18	0.15	0.07
Lean-rich heat exchanger				
Lean in	K	388.87	388.9	389
Lean out	K	331.4	338.9	330.8
Rich in	K	327.91	330.4	321.7
Reboiler temperature	K	385.6	388.0	389.0
Absorber bottom pressure	bar	1.1	1.17	1.16
Absorber top pressure	bar	1.04	1.04	1.04
Desorber bottom (reboiler) pressure	bar	1.71	1.71	1.16
Desorber top pressure	bar	1.69	1.70	1.70
General specifications				
CO_2 capture target	%	91.84	91.85	90
Interstage cooling		Yes	Yes	No

Table 2. Model Validation for GCCmax Solvent[26]

		Data Set 1	Data Set 1	Data Set 2	Data Set 2
Absorber inlet gas stream		Pilot Plant	Simulation	Pilot Plant	Simulation
Nitrogen + Oxygen	Mass fraction	0.895	0.895	0.896	0.896
Carbon dioxide	Mass fraction	0.065	0.065	0.065	0.065
Water	Mass fraction	0.040	0.040	0.039	0.039
Temperature	K	313.1	313.1	312.8	312.8
Total flow rate	kg/s	0.995	0.995	0.9951	0.9951
Absorber					
Absorber top pressure	bara	1.160	1.160	1.160	1.160
Absorber bottom pressure	bara	Unavailable	1.224	Unavailable	1.221
Absorber outlet CO_2 concentration	Mass fraction	0.0053	0.0056	0.004	0.005
Lean solvent–absorber inlet temperature	K	304.1	304.1	325.4	325.4
Rich solvent–absorber outlet temperature	K	318.1	316.5	318.7	316.1
Lean solvent flow rate	kg/s	0.857	0.857	0.756	0.756
Desorber (regenerator)					
Desorber bottom temperature	K	388.6	388.6	395.4	395
Desorber top pressure	bara	1.701	1.708	2.031	2.03
CO_2 stream	kg/s	0.0578	0.0611	0.060	0.0605
Reboiler Steam					
Steam pressure	bar	3.606	3.605	4.075	4.075
Steam temperature	K	402.8	402.8	408.5	408.5
Steam condensate Temperature	K	401.9	401.9	407.8	407.5
Steam flow rate	kg/s	0.091	0.078	0.086	0.0823
Lean-rich heat exchanger temperatures					
Lean solvent in	K	387.4	388.6	394.2	395.0
Lean solvent out	K	325.0	322.6	324.7	327.4
Rich solvent in	K	318.9	316.5	319.9	316.1
Rich solvent out	K	380.4	379.9	384.0	379.9
Lean solvent concentration					
GCCmax solvent	Mass fraction	0.410	0.410	0.439	0.439
Water	Mass fraction	0.536	0.541	0.504	0.515
CO_2	Mass fraction	0.054	0.049	0.057	0.046
General specifications					
CO_2 capture target	%	89.1	91.7	92.50	92.13
Interstage cooling		No	No	No	No

Table 3. Key Process Indicators (KPIs) for the GCCmax Solvent and Baseline MEA Solvent[26]

Key Process Indicators (KPIs)	Unit	MEA	GCCmax (Data1)	GCCmax (Data2)
Heating duty	(MJ/ton CO_2)	3986	2813	2975
Cooling duty	(MJ/ton CO_2)	5644	1524	884
Volume of packing	(m^3/ton CO_2 h^{-1})	46.62	45.64	45.91
Solvent circulation flow rate	(ton solvent/ton CO_2)	34	14	12

different parts of the world, cooling water may be supplied at different temperatures. Again the model predictions are in good agreement with the pilot plant data with respect to the captured CO_2 and the solvent concentrations, giving confidence in the model's predictive capabilities. The discrepancies in the required steam and temperatures were attributed to lack of insulation or temperature measurement errors.

The validated pilot plant model was used to extract several technical key process indicators (KPIs) which are important measures that quantify the difficulties associated with CO_2 separation from the flue gas in terms of the required heating and cooling duties, required packing, and solvent circulation. These measures are scaled with respect to the amount of pure CO_2 captured, to become independent of the pilot plant throughput and enable comparisons. Table 3 shows the KPIs for the baseline solvent (MEA) and the GCCmax solvent.[26] The first indicator is the heating duty, in terms of the required energy needed in the desorber reboiler for separating 1 ton of CO_2. Around 25.4–29.4% reduction in heating duty was observed. Furthermore, a comparison between the values of the second KPI, suggest significant reductions (73–84.4%) in the cooling duties. The third key process indicator is concerned with the volume of packing in the absorber and desorber columns showing improvements in the case of GCCmax solvent. The last KPI is concerned with the required solvent circulations, and is an indicator of the electricity power needed for pumping. The observed improvements are between 58.8–64.7%.

Process scale-up

The validated model was applied for analysis at the large scale corresponding to the retrofitted power plant. The assumptions behind process scale up are summarized in the following. The bulk liquid and gas phases are assumed to be well-mixed at each stage. Phase equilibrium was assumed only at the vapor-liquid interface. It was assumed that the reaction kinetics is significantly faster than the heat and mass transfer rates and therefore, equilibrium chemical reactions sufficiently represent the species composition at the gas-liquid interface. In the present study, the effects of solvent degradation and heat losses were not considered. In practice, for large-scale CO_2 capture processes, achieving the aforementioned performances will require effective gas and liquid distributors. In addition, the process should be carefully insulated and the composition of the solvent should be tightly controlled using makeup.

Solution algorithm: Simulation-optimization framework

The aforementioned problem statement falls into the category of Integrated Process Design and Control (IPDC). The motivation of the integrated approach, as opposed to sequential process design and control design, is due to the fact that when the process design is fixed, there is little room left to improve its operational performance. Therefore, it is highly recommended that operational characteristics should be considered at the early design stages (i.e., process retrofit in the context of this research). A comprehensive review of the methods for IPDC is provided by Sharifzadeh.[20]

The challenge is that the full-space formulation of integrated process and control design for large scale industrial problems such as the abovementioned retrofit problem results in numerically intractable optimization problems. Therefore, an objective of the present research was to identify critical process variables and ensure process operability at the plant-wide level, with a reasonable computational complexity. To this end, a novel simulation-optimization framework was developed and tailored for the aforementioned retrofit problem, as shown in Figure 1 and discussed below.

The proposed optimization framework is shown in Figure 1. Here, the overall process is decomposed into three parts; simulation is used for the power plant and compression plant; optimization is applied to the capture process. These three parts are linked together through flow of materials and energy. As shown in Figure 1, the CO_2 capture process receives the flue gas from the NGCC power plant and depends on the steam supply for regeneration of the solvent. The flow rate of flue gas depends on the electricity power demand and changes as the NGCC power plant experiences variations. In addition, the composition of the flue gas depends on the ratio of the combustion air and natural gas. However, the ratio of combustion air and natural gas is subject to constraints on (1) the maximum allowable temperature of the turbine suction area, and (2) maximum allowable temperature of the turbine discharge gases. Therefore, the operation of CO_2 capture plant is highly entangled with the operational procedure followed for power plant load reduction. As will be shown in the first part of the Results section, the second constraint (i.e., maximum allowable temperature of the turbine discharge gases) becomes active first and by its satisfaction, the first constraint is automatically met.

The variables involved in the optimal design of the CO_2 capture process can be classified as: (1) process design variables and (2) process control variables. The differentiation is necessary as process design variables (such as the dimensions of process equipment) have a physical realization. After the process is commissioned, they are fixed and cannot be changed without costly process modifications. By contrast the control variables (such as the flow rate of the reboiler steam or the circulation rate of the solvent) are available during the process operation to adapt the capture process to the variations in the upstream power plant.

In the proposed optimization framework, without loss of generality, we focus on optimizing the capture plant to manage the numerical size of the problem. The solution algorithm for the optimization framework is as follows:

Algorithm I:

Step (1) The power plant model is run for a series of steady-state electricity load reduction (100%, 75%,

and 50%) scenarios, and a series of default values for the extracted steam and condensate recycle rates. The results of the simulation will determine the flow rate and composition of the flue gas in each scenario.

Step (2) Given the flow rate and composition of the flue gas at various load reduction scenarios, the design and control variables of the capture plant are optimized (as discussed in the following).

Step (3) The results of the optimization determine the optimal values of the extracted steam and recycled condensates. These values are compared to the previous values of the extracted steam and recycled condensates and if the differences are less than the tolerance, the solution is found. Otherwise, the value of the extracted steam and recycled condensates are updated in the power plant model and the algorithm is repeated from Step (1).

Note the compression section does not have mutual interaction with the power plant and capture process. The required energy for CO_2 compression is calculated once the above iterative calculation (Steps 1–3) is converged. In the present study, the economic analysis was concerned only with the capture process. However, the energetic study also studied the interactions between the power plant and capture plant in terms of the required steam and flow rate and composition of the flue gas in addition to the electricity power required for CO_2 compression.

The abstract formulation of the proposed optimization program (blue envelope in Figure 1) is as follows

$$\textbf{Objective} = \boldsymbol{E}(\mathbf{TAC}_s) = \sum_{s=1}^{N_s} \boldsymbol{\mu}_s \times \mathbf{TAC}_s \qquad \textbf{Problem} - 1$$

Subject to

Constraints associated with first principles (transport phenomena, thermodynamics)

Technical Constraints: maximum reboiler temperature (limited by the possibility of solvent degradation)

Control Constraints: 90% CO_2 Capture, maximum turbine discharge temperature

Disturbances: composition and flow rate of flue gas for various power load reduction scenarios

Process design decision variables: the dimensions of absorber, desorber, and heat exchangers

Control (recourse) decision variables: circulation flow rate, reboiler steam flow rate

In the above formulation, $\boldsymbol{E}$ is the expected value, $\boldsymbol{s}$ is the index of the load reduction scenarios, $\boldsymbol{\mu}_s$ is the likelihood of each scenario, and $\boldsymbol{N}_s$ is the total number of scenarios. **TAC** refers to the total annualized cost (TAC) of the capture plant and was calculated as

$$\text{Total Annualized Costs} = \frac{\text{Fixed Capital investment}}{\text{Plant effective Life}} + \text{Total Annual Energy costs} \qquad (1)$$

where the value of 5 years was considered for the capture plant effective life, to combine the plant life and the time value of money. The costs of process equipment were calculated according to the costing correlations provided in.[35] A Lang factor of 6 was considered for estimating the total capital investment.[36] The utility costs considered were 65 \$/MWh for electricity,[37] 0.048 \$/tonne for cooling water,[38] and 14.5 \$/tonne for steam. The MEA solvent loss is around 1400 mg/m^3 of flue gas. Equivalent value for the GCCmax is around 28 mg/m^3. However, as the GCCmax is not priced yet, the costs of solvent losses is not included in the objective function. Solvent degradation was not considered in this study. The considered load reduction scenarios were 100, 75, and 50% and were assumed to be equally likely. As the overall process (Figure 1) consists of two parallel trains, the 50% load reduction in each train will be sufficient to realize a large range of potential operational part-load scenarios (25–100%). The part-load operation of power plants is limited to their turndown ratio (approximately 50%). The turndown ratio is dictated by the technical limitations such as excessive pressure drops across the power plant or the surge margins of the compressor and turbines. In the present research, three operational scenarios were considered; in the first scenario both gas turbines are operated at full load (100%). This scenario refers to the highest conversion efficiency, that is, the highest CO_2 concentration and the smallest steam demand per ton of captured CO_2. In the third scenario, both gas turbines are operated at 50%, which refers to the worst conversion efficiency and hence, the lowest CO_2 concentration and the largest steam demand per ton of captured CO_2. The second scenario is intermediate, where both gas turbines are operated at 75%. These scenarios cover all the operating regions thoroughly. It is notable that there are other operating scenarios where the gas turbines could be operated at different loads (e.g., operating one of trains at full load and shutting down the other), which could be more energy efficient. However, the aforementioned scenarios are more comprehensive with respect to CO_2 concentration and flow rate.

From the optimization programming point of view, the above formulation conforms to a two-stage recourse-based optimization under uncertainty.[39] From the Control Engineering point of view, the above formulation conforms to a steady-state inversely controlled process model (ICPM).[40,41] Here the treatment is based on the property that the inverse solution of process model can be applied to evaluate the best achievable control performance. The idea is shown in Figure 4, adapted from Ref. 41. In a steady-state ICPM, the values for the manipulated variables (MVs) required for maintaining the controlled variables (CVs) at constant setpoints are calculated using the inverse of process model. As discussed by Sharifzadeh[20,41] using this strategy, it is possible to ensure that the process remains operable under various disturbance scenarios (i.e., electricity load reduction). It is notable that application of a *dynamic* ICPM[42] also enables studying the process controllability during transient states. However, we defer such detailed analysis to our future research. In the context of the present study concerning carbon capture from the NGCC power plant, two model inversions were conducted. First, the temperature of the turbine discharge gases (as discussed and justified later in the result section) is chosen as the controlled variable (CV). The corresponding MV is the flow rate of the combustion air, which is varied to maintain the temperature of the turbine discharge gases constant at its maximum allowable value. The second CV was the CO_2 capture target. Here, the corresponding MVs are the reboiler steam flow rate and the solvent circulation rate which are optimally varied to keep the CV at the 90% CO_2 capture target. It is notable that in the context of present study, the NGCC power plant model is applied to derive realistic disturbance scenarios (red envelop in Figure 4) in terms of the flow rate and composition of the

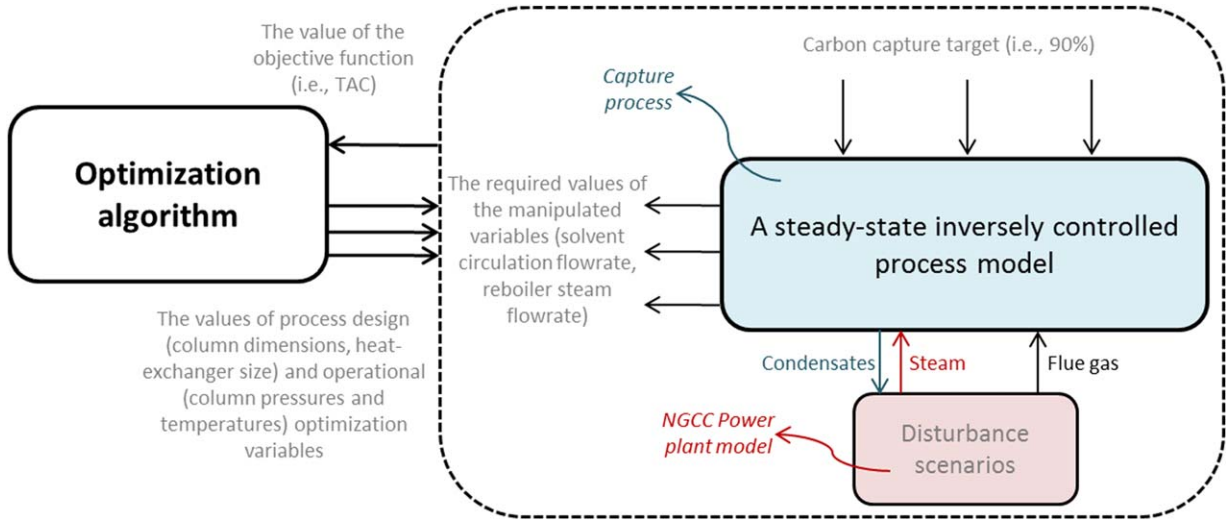

Figure 4. Optimizing a steady-state inversely controlled process model, adapted from.[40]

[Color figure can be viewed in the online issue, which is available at wileyonlinelibrary.com.]

flue gas for the carbon capture process. The challenge is that there are mutual interactions between the capture process and the power plant, shown by arrays in Figure 4. While the steam needed for solvent regeneration depends on the flow rate and composition of the flue gas, the overall fuel consumption and hence the flue gas itself, also depends on the required steam in the desorber reboiler. In the present study, such mutual interactions is captured using the iterative steps in Algorithm I, as outlined earlier.

Model development and implementation software tools

The NGCC power plant and compression process were modeled in gCCS,[43] a software tool developed by PSE. The specification of the NGCC power plant model was received from PSE from one of their earlier industrial projects. The important characteristics of the developed model were calculation of the efficiency of the compressors and turbines using performance curves and calculation of material flow rates based on pressure differences. The capture plant model was developed using the Advanced Model Library for GLC (AML:GLC)[44] and gSAFT.[45] As described extensively earlier, the main characteristics of the capture process model were rate-base modeling of mass and heat transfer phenomena and representation of chemisorption reactions using SAFT equation of state. The heat-exchangers were modeled using gCCS in the *operational* mode. The implication is that the surface area was an optimization variable, and given the heat transfer coefficient, the temperatures of the hot and cold streams were calculated. In the present study, the gPROMS default values for the solution parameters were used (e.g., 10^{-5} for absolute tolerance). Similar to other NLP algorithms, the solution time depends on the initial guess for the optimization variables, and typically takes 1–2 days to converge.

Results of Optimization Programming

The Results Section is organized as follows. First, it is investigated how the CCGT control strategy influences the flue gas composition and flow rate. These discussions enable underpinning the interactions between the power plant and capture process during electricity load reduction scenarios.

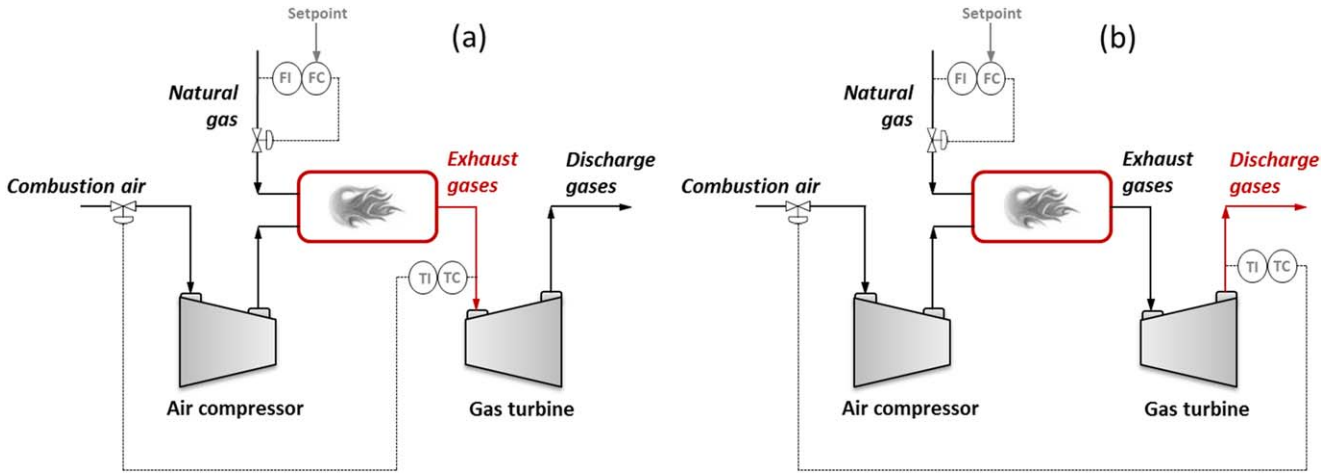

Figure 5. The Control structure for combined cycle gas turbine (CCGT) during power plant load reduction: (a) the temperature of combustor exhaust gases is controlled (b) the temperature of turbine discharge gases is controlled.

[Color figure can be viewed in the online issue, which is available at wileyonlinelibrary.com.]

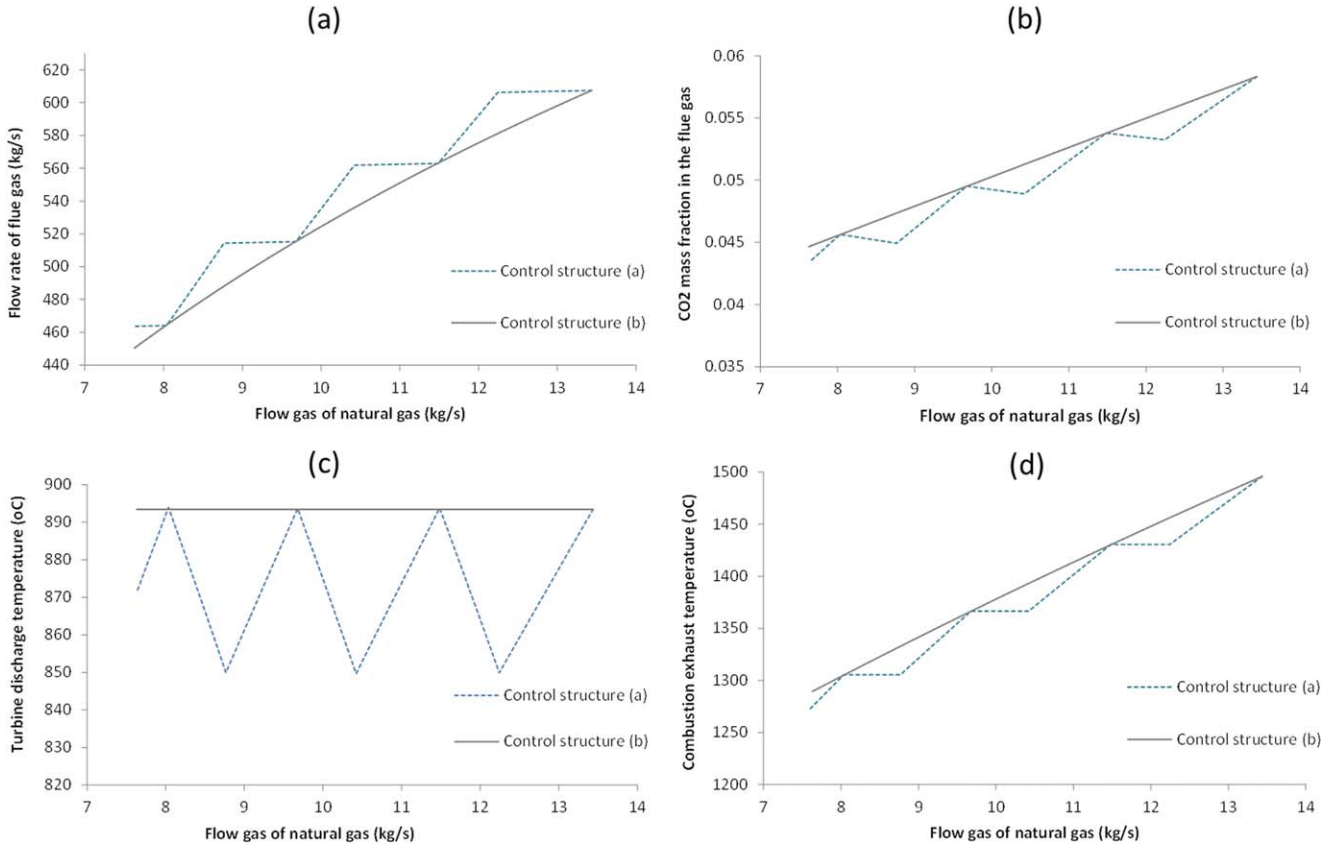

Figure 6. The flow rate of flue gas (a), The CO_2 mass fraction of flue gas (b), the temperature of turbine discharge gases (c) and the temperature of combustion exhaust gases (d) for the control structures (a) and (b) in Figure 5.

[Color figure can be viewed in the online issue, which is available at wileyonlinelibrary.com.]

Then, the results of the optimization Problem 1 are reported and discussed. Finally, the implications of NGCC power plant retrofit and integration with capture plant for the overall energy conversion are evaluated and discussed.

Control strategy for CCGT

This section discusses the operation of CCGT at steady state, which has profound implications for the flow rate and composition of the flue gas. When the power plant is operated at full load, the ratio of the combustion air and natural gas flow rates is adjusted to maximize energy conversion. However, as the electricity power demand is reduced, the flow rate of natural gas is reduced accordingly and maintaining a constant ratio with combustion air flow rate would increase the temperature of the combustor exhaust gases and turbine discharge gases which could potentially damage the process equipment. Therefore, a control strategy is needed that systematically safeguards the process equipment.

In practice, there are two control structures in use,[46] shown in Figures 5a, b. Both control structures have a similar control

Table 4. The Results of Flexible Operation of NGCC Power Plant for Various Electricity Load, with and Without CO_2 Capture and Compression Plants: GCCmax Solvent

		Nominal[a]	100% Load	75% Load	50% Load
NG flow rate[b]	kg/s	26.87	26.87	21.08	15.25
Flue gas flow rate	kg/s	1214.8	1214.8	1022.6	801.5
Flue gas composition: N_2	Mass fraction	0.7601	0.7601	0.7611	0.7623
Flue gas composition: O_2	Mass fraction	0.1169	0.1169	0.1230	0.1294
Flue gas composition: H_2O	Mass fraction	0.0647	0.0647	0.0615	0.0581
Flue gas composition: CO_2	Mass fraction	0.0583	0.0583	0.0544	0.0502
Generated power in NGCC[b]	MW	747.18	698.78	510.43	341.75
Extracted steam[b]	kg/s	–	68.24	52.4	36.76
Power consumed in compressors[b]	MW	–	20.68	15.88	11.64
Net produced electricity[b]	MW	747.18	678.1	494.55	330.1
Energy content of feed (HHV)[b]	MW	1292.62	1292.62	1014.07	733.66
CO_2 captured	kg/s	63.74	63.74	50.07	36.20
Electricity costs	$/MWh	65.00	71.62	77.04	83.50
Overall conversion efficiency	%	57.8	52.46	48.77	44.99

[a]Nominal refers to the standalone scenario where the power plant is operated at its nominal operating point without CO_2 capture and compression plants.
[b]The reported flow rates and power values are for the overall process and include the two trains of CCGT, HRSG, CO_2 capture and compression sections.

Table 5. The Results of Flexible Operation of NGCC Power Plant for Various Electricity Load, with and Without CO_2 Capture and Compression Plants: MEA Baseline Solvent

		Nominal[a]	100% Load	75% Load	50% Load
NG flow rate[b]	kg/s	26.87	26.87	21.08	15.25
Flue gas flow rate	kg/s	1214.8	1214.8	1022.6	801.5
Flue gas composition: N_2	Mass fraction	0.7601	0.7601	0.7611	0.7623
Flue gas composition: O_2	Mass fraction	0.1169	0.1169	0.1230	0.1294
Flue gas composition: H_2O	Mass fraction	0.0647	0.0647	0.0615	0.0581
Flue gas composition: CO_2	Mass fraction	0.0583	0.0583	0.0544	0.0502
Generated power in NGCC[b]	MW	747.18	679.94	495.89	331.09
Extracted steam[b]	kg/s	–	98.12	77.16	54.59
Power consumed in compressors[b]	MW	–	20.68	15.88	11.64
Net produced electricity[b]	MW	747.18	659.26	480.01	319.45
CO_2 captured	kg/s	63.74	63.74	50.07	36.20
Energy content of feed (HHV)[b]	MW	1292.45	1292.45	1013.95	733.53
Electricity costs	$/MWh	65.00	73.67	79.38	86.29
Overall conversion efficiency	%	57.8	51.01	47.34	43.55

[a]Nominal refers to the standalone scenario where the power plant is operated at its nominal operating point without CO_2 capture and compression plants.
[b]The reported flow rates and power values are for the overall process and include the two trains of CCGT, HRSG, CO_2 capture and compression sections.

loop in that, the setpoint of the natural gas flow controller is adjusted according to the electricity power demand. However, the two control structures differ in the selected CV in the second control loop. In the first control structure (Figure 5a), the temperature of the combustor exhaust gases is controlled. By comparison, in the second control structure (Figure 5b), the temperature of the turbine discharge gases is controlled. The first control strategy requires a recurrent procedure. The reason is that maintaining the temperature of the combustor exhaust gases at a constant value results in an increase in the temperature of the turbine discharge gases that can damage the downstream HRSG section. Therefore, the operational strategy in the first control structure consists of two iterative control modes:

Mode (i): The flow rate of the natural gas is reduced while the flow rate of the combustion air is maintained constant (dotted line in Figure 6a). This results in a reduction in the temperature of the turbine discharge gases (descending dotted line in Figure 6c).

Table 6. The Results of GCCmax Solvent for Various Load Reduction Scenarios (All the Results are Reported for One Train)

		50% Load	75% Load	100% Load
Absorber				
Diameter	m	13.58	13.58	13.58
Length	m	12.47	12.47	12.47
Absorber top pressure	Pa	1.29 E +05	1.18 E +05	1.03 E +05
Absorber bottom pressure	Pa	1.35 E +05	1.35 E +05	1.35 E +05
Lean Solvent to absorber				
Flow rate	kg/s	840.622	1139.86	1383
Temperature	K	313.15	313.15	313.15
Water	Mass fraction	0.5036	0.5036	0.5036
CO_2	Mass fraction	0.0864	0.0864	0.0864
GCCmax	Mass fraction	0.4100	0.4100	0.4100
Lean-Rich Heat Exchanger				
Area	m^2	69,398	69,398	69,398
Lean inlet temperature	K	384.3	384.3	384.3
Lean outlet temperature	K	328.1	329.5	330.8
Rich inlet temperature	K	327.0	327.9	328.4
Rich outlet temperature	K	383.9	383.4	382.8
Desorber				
Diameter	m	6.59	6.59	6.59
Length	m	6.11	6.11	6.11
Reboiler				
Reboiler temperature	K	384.3	384.3	384.3
Reboiler pressure	Pa	2.21×10^5	2.21×10^5	2.21×10^5
Stream flow rate	kg/s	18.38	26.20	34.12
Steam inlet pressure	Pa	3.61×10^5	3.61×10^5	3.61×10^5
Steam inlet temperature	K	402.8	402.8	402.8
Condenser temperature	K	313.15	313.15	313.15
Lean solvent cooler temperature	K	313.15	313.15	313.15
Carbon capture target	%	90.0	90.0	90.0
Key process indicators (KPIs)				
Packing volume	m^3/(tonne CO_2 hr)	30.9	22.4	17.5
Heating duty	MJ/tonne CO_2	2166	2251	2348
Cooling duty	MJ/tonne CO_2	1990	2179	2305
Circulation rate	ton solvent/tonne CO_2	46.7	46.5	45.7
Total Purchased Equipment costs	$	8.47×10^6	8.47×10^6	8.47×10^6
Annualized energy costs	$/year	1.13×10^7	1.62×10^7	2.13×10^7
Total annualized costs (TACs)	$/year	2.15×10^7	2.63×10^7	3.15×10^7

Table 7. The Results of MEA Baseline Solvent for Various Load Reduction Scenarios (All the Results are Reported for One Train)

		50% Load	75% Load	100% Load
Absorber				
Diameter	m	14.99	14.99	14.99
Length	m	14.75	14.75	14.75
Absorber top pressure	Pa	1.28 E +05	1.20 E +05	1.03 E +05
Absorber bottom pressure	Pa	1.35 E +05	1.35 E +05	1.35 E +05
Lean Solvent to absorber				
Flow rate	kg/s			
Temperature	K	313.9	313.9	313.9
Concentration				
Water	Mass fraction	0.6504	0.6504	0.6504
MEA	Mass fraction	0.2820	0.2820	0.2820
CO_2	Mass fraction	0.0676	0.0676	0.0676
Lean-rich heat exchanger				
Area	m^2	60,174.5	60,174.5	60,174.5
Lean inlet temperature	K	388.6	388.6	388.7
Lean outlet temperature	K	332.7	334.3	334.3
Rich inlet temperature	K	326.8	327.7	327.9
Rich outlet temperature	K	384.3	382.7	381.6
Desorber				
Diameter	m	11.47	11.47	11.47
Length	m	10.20	10.20	10.20
Reboiler				
Reboiler temperature	K	388.6	388.6	388.7
Reboiler pressure	Pa	1.85×10^5	1.85×10^5	1.85×10^5
Stream flow rate	kg/s	27.30	38.58	49.06
Steam inlet pressure	Pa	3.05×10^5	3.05×10^5	3.05×10^5
Steam inlet temperature	K	400.6	400.6	400.6
Condenser temperature	K	313.9	313.9	313.9
Lean solvent cooler temperature	K	313.9	313.9	313.9
Carbon capture target	%	90.0	90.0	90.0
Key process indicators (KPIs)				
Packing volume	m^3/(tonne $CO_2 \times$ h)	55.95	40.7	32.2
Heating duty	MJ/tonne CO_2	3241.2	3329.9	3348.2
Cooling duty	MJ/tonne CO_2	4754.6	4991.7	4998.2
Circulation rate	ton solvent/tonne CO_2	53.1	51.6	49.3
Total purchased equipment costs	$	8.28×10^6	8.28×10^6	8.28×10^6
Annualized energy costs	$/year	1.54×10^7	2.18×10^7	2.76×10^7
Total annualized costs (TACs)	$/year	2.64×10^7	3.31×10^7	3.91×10^7

Mode (ii): The temperature of combustion exhaust gases is controlled using the combustion air flow rate (constant dotted line in Figure 6d) as the flow rate of the natural gas is further reduced. This results in an increase (ascending dotted line in Figure 6c) in the temperature of the turbine discharge gases until it reaches a limit where there is a risk of thermal shock to the downstream equipment. The control system switches to Mode (i).

Unlike the first control strategy, the second control strategy requires only one operational mode. The reason is that by controlling the temperature of the turbine discharge gases (solid line in Figure 6c) the temperature of combustion exhaust gases decreases (solid line in Figure 6d). In other words, the constraint on the turbine discharge temperature becomes active first and automatically satisfies the constraint on the combustion exhaust temperature. Figures 6a, b suggest that the second control strategy is optimal with respect to the CO_2 separation as it produces less flue gas with a higher CO_2 content, that is, easier carbon capture task.

Overall energy conversion efficiency and implications of carbon capture and compression

Table 4 reports the results summary for the scenario in which the capture process is operate with the GCCmax solvent. The features of interest include the flow rate of natural gas feed, the flow rate and composition of the flue gas, the generated power, the required steam for solvent regeneration, the power needed for CO_2 compression, the cost of produced electricity, and the overall energy efficiency. Similar results are reported in Table 5 where the MEA reference solvent is used. In both scenarios, the flow rate of natural gas is gradually reduced from the nominal value of 26.87 kg/s by almost 50% and the design and operation of the capture plant are optimized according to the simulation-optimization framework shown in Figure 1. These tables exhibit common observations regarding the implications of electricity load reduction for power generation with CO_2 capture. In all scenarios, CO_2 capture and compression impose energetic penalties in terms of the required steam for solvent regeneration and the electric power needed for CO_2 compression. In addition, as the electricity load is decreased, the energy conversion efficiency is reduced, due to the reduced efficiency of process equipment such as turbines and compressors. The combination of these penalties reduces the net produced electricity and decreases the overall energy efficiency.

The implications of load reduction for operation of the capture plant are more convoluted. To enable the discussions more details are provided in Tables 6 and 7, which report the design and operational specifications for the load reduction

scenarios, in the case of GCCmax and MEA solvents, respectively. As the electricity load is reduced, the concentration of CO_2 in the flue gas (Tables 4 and 5) decreases, which suggests a more difficult separation task. On the contrary, more contact area (shown by packing volume KPI in Tables 6 and 7) becomes available between the gas and liquid phases. Then, it is for the optimization algorithm to adjust the solvent circulation rate and reboiler steam for each electricity load scenario and establish a trade-off between the capital investment and the energy costs. Overall, a minor decrease in the heating and cooling indicators and solvent circulation indicators are observed for load reduction scenarios. Another important feature of interest is the design and operation of the absorber column. The absorber experiences the largest variations during load reduction due to drastic variations in the flue gas flow rates. While the desired extent of CO_2 capture constrains the required gas-liquid contact area, a tall/thin column would result in very HP drops at full load operation and a short/fat column would result in channelling during part-load operation. Therefore, it was for the optimization algorithm to find a compromise design that satisfies the CO_2 capture constraint and ensures process operability in all load reduction scenarios. Tables 6 and 7 suggest that the optimized columns were neither fat nor thin but almost square. The justification for the large heat transfer areas is the fact that the overall economy is governed by the required reboiler steam. Such a large heat transfer area may require special equipment such as plate heat exchangers. As the heat-transfer area was the same in all scenarios, the approach temperatures are smaller in part-load scenarios as less solvent is circulated. Finally, a comparison between the KPIs in Tables 6 and 7 suggests that GCCmax features superior performance as it required 45% less column packing, 30% less steam, 54% less cooling water, and 7% less pumping energy (shown by solvent circulation rate), per unit mass of captured CO_2. The estimated total annualized costs of the capture process at full load were 3.15×10^7 \$/year and 3.91×10^7\$/year for GCCmax and MEA solvents, respectively.

Conclusions

The present research studied scale up and integration of a solvent-based carbon capture process into a NGCC power plant for a novel solvent, GCCmax, and the MEA reference solvent. The aim was to establish and quantify the superior performance of the new solvent at an industrial scale. Furthermore, the present research provided in-depth insights into retrofit and flexible operation of NGCC power plants. It was observed that the control strategy for the CCGT during load reduction, has profound implications for the flow rate and composition of flue gas, and hence affects carbon capture costs. It was also observed that NGCC power plants are less efficient at part-load operational scenarios. In the present research, the method of IPDC was adapted and solved. The proposed optimization algorithm successfully established a trade-off between the design and operational criteria. The overall total annual costs in terms of capital investment and energy costs were minimized while the process operability was ensured under all load-reduction scenarios.

As comparison between various economic analysis available in open literature is challenging due to different scope of system analysis, modeling details and the economic estimation methods, and in the absence of economic data from industrial-scale demonstration plants, the present study chose to apply a set of KPIs enabling objective and reproducible comparisons. In all scenarios, the GCCmax performed better KPIs than the MEA reference solvent. GCCmax belongs to the family of the APBS solvents. It features a lower heat of absorption compared to MEA and its kinetics is enhanced by a buffer salt. This combination enables GCCmax to require less regeneration energy and to feature a higher CO_2 loading, resulting in a superior performance compared to the MEA benchmarks. While the comparative study was tailored to the aforementioned solvents, the research methodology is generic and provides effective standards and benchmarking criteria for new solvent development.

Acknowledgments

The authors would like to acknowledge the financial support by Carbon Clean Solutions (CCSL) under UK-Department of Energy & Climate Change (DECC) grant. The authors are also thankful to Process Systems Enterprise Ltd (PSE) for technical support and providing modeling libraries.

Literature Cited

1. International Energy Agency (IEA). *World Energy Outlook*. Paris: International Energy Agency (IEA), 2014.
2. Bottoms RR. Process for Separating Acidic Gases. US patent 1,783,901, 1930.
3. International Energy Agency (IEA). *Retrofit of CO_2 Capture to Natural Gas Combined Cycle Power Plants*. IEA Greenhouse Gas R&D Programme. Report number 2005/1. Paris, Jan 2005. Available at: http://www.ieaghg.org/docs/General_Docs/Reports/2005-1.zip.
4. Haslbeck L, Kuehn NJ, Lewis EG, Pinkerton LL, Simpson J, Turner MJ, Varghese E, Woods MC. *Cost and Performance Baseline for Fossil Energy Plants, Volume 1: Bituminous Coal and Natural Gas to Electricity. Revision 2*. Pittsburgh, PA: National Energy Technology Laboratory (NETL). Report number DOE/NETL-2010/1397, Nov 2010.
5. Manzolini G, Sanchez Fernandez E, Rezvani S, Macchi E, Goetheer ELV, Vlugt TJH. Economic assessment of novel amine based CO_2 capture technologies integrated in power plants based on European Benchmarking Task Force methodology. *Appl Energy*. 2015;138:546–558.
6. Lucquiaud M, Gibbins J. On the integration of CO_2 capture with coal-fired power plants: a methodology to assess and optimise solvent-based post-combustion capture systems. *Chem Eng Res Des*. 2011;89:1553–1571.
7. Romeo LM, Bolea I, Lara Y, Escosa JM. Optimization of intercooling compression in CO_2 capture systems. *Appl Therm Eng*. 2009;29:1744–1751.
8. Karimi M, Hillestad M, Svendsen HF. Capital costs and energy considerations of different alternative stripper configurations for post combustion CO_2 capture. *Chem Eng Res Des*. 2011;89:1229–1236.
9. Pfaff I, Oexmann J, Kather A. Optimised integration of post-combustion CO_2 capture process in greenfield power plants. *Energy*. 2010;35:4030–4041.
10. Jonshagen K, Sipöcz N, Genrup M. A novel approach of retrofitting a combined cycle with post combustion CO_2 capture. *J Eng Gas Turbine Power*. 2010;133:011703–011703-7. Available at: http://gasturbinespower.asmedigitalcollection.asme.org/article.aspx?articleid=1425741&resultClick=3.
11. Khalilpour R, Abbas A. HEN optimization for efficient retrofitting of coal-fired power plants with post-combustion carbon capture. *Int J Greenhouse Gas Control*. 2011;5:189–199.
12. Biliyok C, Yeung H. Evaluation of natural gas combined cycle power plant for post-combustion CO_2 capture integration. *Int J Greenhouse Gas Control*. 2013;19:396–405.
13. Luo X, Wang M, Chen J. Heat integration of natural gas combined cycle power plant integrated with post-combustion CO_2 capture and compression. *Fuel*. 2015;151:110–117.
14. Li H, Ditaranto M, Berstad D. Technologies for increasing CO_2 concentration in exhaust gas from natural gas-fired power production

with post-combustion, amine-based CO_2 capture. *Energy*. 2011;36: 1124–1133.
15. Oyenekan BA, Rochelle GT. Energy performance of stripper configurations for CO_2 capture by aqueous amines. *Ind Eng Chem Res*. 2006;45:2457–2464.
16. Le Moullec Y, Neveux T, Al Azki A, Chikukwa A, Hoff KA. Process modifications for solvent-based post-combustion CO_2 capture. *Int J Greenhouse Gas Control*. 2014;31:96–112.
17. Ahn H, Luberti M, Liu Z, Brandani S. Process configuration studies of the amine capture process for coal-fired power plants. *Int J Greenhouse Gas Control*. 2013:16;29–40.
18. Damartzis T, Papadopoulos AI, Seferlis P. Process flowsheet design optimization for various amine-based solvents in post-combustion CO_2 capture plants. *J Clean Prod*. 2015; In press. doi:10.1016/j.jclepro.2015.04.129.
19. Karimi M, Hillestad M, Svendsen HF. Investigation of the dynamic behavior of different stripper configurations for post-combustion CO_2 capture. *Int J Greenhouse Gas Control*. 2012;7:230–239.
20. Sharifzadeh M. Integration of process design and control: a review. *Chem Eng Res Des*. 2013;91:2515–2549.
21. Mac Dowell N, Shah N. The multi-period optimisation of an amine-based CO_2 capture process integrated with a super-critical coal-fired power station for flexible operation. *Comput Chem Eng*. 2015;74: 169–183.
22. Delarue E, Martens P, D'haeseleer W. Market opportunities for power plants with post-combustion carbon capture. *Int J Greenhouse Gas Control*. 2012;6:12–20.
23. Lawal A, Wang M, Stephenson P, Obi O. Demonstrating full-scale post-combustion CO_2 capture for coal-fired power plants through dynamic modelling and simulation. *Fuel*. 2012;101:115–128.
24. Chalmers H, Gibbins J. Initial evaluation of the impact of post-combustion capture of carbon dioxide on supercritical pulverised coal power plant part load performance. *Fuel*. 2007;86: 2109–2123.
25. Cohen SM, Rochelle GT, Webber ME. Optimal operation of flexible post-combustion CO_2 capture in response to volatile electricity prices. *Energy Procedia*. 2011;4:2604–2611.
26. Sharifzadeh M, Shah, N. Comparative studies of CO_2 capture solvents for gas-fired power plants: integrated modelling and pilot plant assessments. *Int J Greenhouse Gas Control*; in press. DOI: 10.1016/j.ijggc.2015.10.009.
27. Seader JD, Henley EJ, Roper DK. *Separation Process Principles*, 3rd ed. Hoboken: John Wiley & Sons, Inc., 2013.
28. Onda K, Takeuchi H, Okumoto Y. Mass transfer coefficients between gas and liquid phases in packed columns. *J Chem Eng Jpn*. 1968;1:56–62.
29. Bravo JL, Fair JR. Generalized correlation for mass transfer in packed distillation columns. *Ind Eng Chem Process Des Dev*. 1982; 21:162–170.
30. Billet R, Schultes M. Predicting mass transfer in packed columns. *Chem Eng Technol*. 1993;16:1–9.
31. Bravo JL, Rocha JA, Fair JR. Mass transfer in Gauze Packings. *Hydrocarbon Process*. 1985;64:56–60.
32. Bravo JL, Rocha JA, Fair JR. A comprehensive model for the performance of columns containing structured packings. *Inst Chem Eng Symp Ser*. 1992;128:A489–A507.
33. Mac Dowell N, Samsatli NJ, Shah N. Dynamic modelling and analysis of an amine-based post-combustion CO_2 capture absorption column. *Int J Greenhouse Gas Control*. 2013;12:247–258.
34. Mac Dowell N, Llovell F, Adjiman CS, Jackson G, Galindo A. Modeling the fluid phase behavior of carbon dioxide in aqueous solutions of monoethanolamine using transferable parameters with the SAFT-VR approach. *Ind Eng Chem Res*. 2010;49:1883–1899.
35. Couper JR, Penney WR, Fair JR. *Chemical Process Equipment Selection and Design*, 3rd ed. Burlington: Elsevier Science, 2012.
36. Peters MS, Timmerhaus KD, West RE. *Plant Design and Economics for Chemical Engineers*, 5th ed. London: McGraw-Hill Chemical Engineering Series, 2003.
37. Energy Information Administration. *Electricity wholesale market*. Washington DC: US Department of Energy. Available at: http://www.eia.gov/electricity/wholesale/. Accessed 15 September 2015.
38. Ulrich GD, Vasudevan PT. How to estimate utility costs. *Chem Eng*. 2006;113:66–69.
39. Grossmann IE. Advances in mathematical programming models for enterprise-wide optimization. *Comput Chem Eng*. 2012;47:2–18.
40. Sharifzadeh M, Thornhill NF. Optimal selection of control structures using a steady-state inversely controlled process model. *Comput Chem Eng*. 2012;38:126–138.
41. Sharifzadeh M. Implementation of a steady-state inversely controlled process model for integrated design and control of an ETBE reactive distillation. *Chem Eng Sci*. 2013;92:21–39.
42. Sharifzadeh M, Thornhill NF. Integrated design and control using a dynamic inversely controlled process model. *Comput Chem Eng*. 2013:48:121–134.
43. *gCCS: Whole chain CCS systems modelling software tool*. London: Process Systems Enterprise. Available at: http://www.psenterprise.com/power/ccs/gccs.html. Accessed 15 September 2015.
44. *Advanced Model Library - Gas-Liquid Contactors (AML:GLC) software tool*. London: Process Systems Enterprise. Available at: http://www.psenterprise.com/processbuilder/libraries/aml_glc.html. Accessed 15 September 2015.
45. *gSAFT software tool*. London: Process Systems Enterprise. Available at: http://www.psenterprise.com/gproms/options/physprops/saft/. Accessed 15 September 2015.
46. Weber PT. *Modeling gas turbine engine performance at part-load. A Thesis for UTSR Gas Turbine Industrial Fellowship Program*. Electric Power Research Institute, Southwest Research Institute, University of Wyoming. Available at: http://www.swri.org/utsr/presentations/WeberPatrickRept.pdf. Accessed 15 September 2015.

Manuscript received May 16, 2015, and revision received Oct. 6, 2015.